Journal of Academic and Applied Studies
(Special Issue on Applied Sciences)
Vol. 3(9) September 2013, pp. 22-37
Available online @ www.academians.org

ISSN1925-931X

Petrography and Petrogenesis of the Neshveh Intrusive Rocks, Northeast Saveh, Central Iran

Amin panahi[1], Reza Keshavarzi[2], Masood kiani[3], Mansor Taheri[4], Bahman Javadian[3]

[1]*Department of geology, North Tehran Branch, Islamic Azad University , Iran*

[2]*Department of Geology ,University of Tehran, Iran*

[1]*Department of geology, Science and Research Branch, Islamic Azad University, Iran*

[4]*Department of Geology , Shahid Chamran University Ahwaz, Iran*

Abstract
The Neshveh intrusive mass is located in the Northeast of Saveh and is considered as a part of the Urumieh-Dokhtar magmatic arc (UDMC). The mass is replaced in the Eocene-Oligocene volcanosedimentary rocks consist mainly of quartz monzodiorite, granodiorite and granite. Based on the Field studies, petrographical and geochemical evidences, the Neshveh rocks have derived from a K-rich, metaluminous calc-alkline magma. P_2O_5 versus SiO_2 has a decreasing trend that is a sign of I-type rocks. Due to entrance into the structure of minerals like: Fe-Ti oxides, plagioclase and hornblende, MgO, Fe_2O_3, MnO, Al_2O_3 and TiO_2decrease with increasing SiO_2. On the other hand Rb and Ba increasing trend demonstrate no fractionation of biotite and K-feldspar during the magma evolution. Y decreasing trend results from fractionation of hornblende. REE patterns of the studied rocks normalized by Chondrite, follow same trend representing their unity source and the role of the fractionation in the magma evolution. Low amounts of some elements such as; V, Co, Cr, Ni, Mg# in Neshveh intrusive rocks reveal their formation from an evolved magma.

Key words : Saveh- Neshveh-petrography-geochemistry

I. Introduction

Early studies on Saveh area set out by Kaya et al (1978), Dehlavi (1978) and Helmi (1991) focused mainly on petrography and petrochemistry of the volcanic and plutonic rocks in the study area. According to Moeinvaziri (1999) the Neshveh volcanic rocks in the northwest of Saveh comprise as several groups: riolith, dacite and in lesser amount andesite that are the oldest rocks in the area; pyroclastic and flow lavas with intercalated marl, sandstone and lutetian limestones; and priabonian andesitic and latitic lavas with porphyritic texture laid above all (Fig. 1). The Eocene volcanic rocks are widespread in the study area and derived mostly from crustal-

Journal of Academic and Applied Studies
(Special Issue on Applied Sciences)
Vol. 3(9) September 2013, pp. 22-37
Available online @ www.academians.org

ISSN1925-931X

mantle sources. The two sources of these rocks attributed to rising of a mantle-derived basic magma and assimilation of the continental crust.

The Neshveh intrusive mass situated between 35º10' and 35º 14' north latitudes and 50º 10' and 50º 14' east longitudes 40 km from northwest of Saveh considered as a part of the UMDC. Since no tenuous petrographical and geochemical studies has been made on these rocks, this paper set out to realize the petrology, tectonic setting and major and trace element variations.

Geology

Tectonic elements in the west and southwest of Iran can be categorized as; 1) Uromieh-Dokhtar Magmatic Arc (UDMC), 2) Sanadaj-Sirjan Zone and 3) Zagros Fold-Thrust Belt (Alavi, 1994).

The UDMC consists Eocene-Quaternary volcanic and plutonic rocks as long as 50 km and 4 km thicknesses (Berberian and King, 1981). The Eocene volcanic rocks are the most abundant.

The Uromieh-Dokhtar igneous rocks have various Chemical and petrological composition from acidic to basic and so formation environments from continental to marine low depth. Among these, the acidic igneous masses are in abundant compared with medium to basic rocks and mostly formed due to continental crust melting (Stokline, 1981).

Saveh area is a part of the UDMC located in the central iran. The UDMC is a part of the Alpe-Himalayan orogenic belt and situated between Eurasian and Arabian tectonic plates in same trend with Sanandaj-Sirjan metamorphosed zone (NW-SE trend). The magmatism of this belt is a matter of debate, assome of the investigators (e.g. Caillat, 1978; Emami, 1981) relate it to the intracontinental rifts, while others (e.g. Berberian& King, 1981; Alavi, 1994 ;Moenvaziri, 1999 ;Shahabpour, 2007) propose the subduction of the Neotethyan oceanic lithosphere beneath the central Iranian plate as the reason of the magmatism in this belt.

Petrography:

The Neshveh intrusive mass with area about 56 km^2has an East-West trend. Its long appearance probably caused from the role of the faults in magma ascension. The mass has crossed by some andesitic dykes.

In order to petrographical studies after accurate sampling, about 87 thin sections were provided. The studied rocks comprise quartzmonzodiorite to granite (Fig. 2). The main texture of the mass is medium to course granular and locally porphyroidal with plagioclase phenocrysts, microgranular and graphical textures are visible.

The granodiritic rocks composed mainly of plagioclases (43.38%), quartz (19.78%), alkali feldspars (17.38%), biotite (4.4%), other ferromagnesian minerals (11.13%) and opaque (2.14%),are the most abundant in the mass (table 1).

The granitic rocks with granular and medium grains textures and in lesser amount porphiroidal with plagioclase phenocrysts are the next abundant rocks formed in the margin of the mass. The main minerals in these rocks are; plagiocalse (37.3%), quartz (26.5%) and alkali

Journal of Academic and Applied Studies
(Special Issue on Applied Sciences)
Vol. 3(9) September 2013, pp. 22-37
Available online @ www.academians.org

ISSN1925-931X

feldspar (28%). Amphiboles (5.5%), opaques (1.5%) and biotites (1%) can be assumed as accessory mineral phases (table 1).

Plagioclase minerals are euhedral and subhedral with polycinthetic macle in the studied mass that some of them are sericitized. Orthoclase with Carlsbad macle is the main alkali feldspar altered to clay minerals in some sections. Quartz as intercertal, fine grained to medium and unhedral mineral in these rocks, has oscillary In some thin sections, clinopyroxenes are completely replaced by actinolithes especially in quartz-monzodiorite with porphyry texture. Accessory minerals in the Neshveh intrusive mass are dominantly; amphibole, opaque, biotite, zircon and sphene. Sericite, epidote, actinolithe, chlorite and clay minerals are accounted as secondary minerals. Fe-Mg bearing minerals are mostly amphibole and in a lesser amount biotite in the mass. Amphibole crystals have dark green color with cleavages through the crystal lengths.

Geochemistry:

To investigate geochemical of the Nevaeh intrusive rocks, 8 samples from diverse lithological units were selected and sent to the ALS Cheema laboratory in the Canada for elemental analysis. The results are represented in table (1). It has been tried to decipher the magmatic evolutions during the formation of these rocks using metrological diagrams and elemental arrays.

Based on the K_2O versus SiO_2 diagram, the studied rocks have high-K calk-alkaline nature (Fig 3) confirms by their linear trend in the AFM diagram (Fig 4).

On the other hand, using A/CNK and A/NK diagrams, the studied samples fall in the metaluminous field (Fig 5).Based on the Na_2O/K_2O ratio (more than 1), these rocks can be considered as sodic.

The SiO_2amounts of these rocks are various from 56.5 to 69.4 that reveals their lithological diversity (table 2). SiO_2 versus major element variations are shown in Figure (6). As it can be observed increasing SiO_2, results decreasing AL_2O_3, P_2O_5, CaO, TiO_2, MgO, MnO and Fe_2O_3 and so Sr, Cr, Ni and Y while K_2O, Na_2O and so Rb, Th, Ba, Zr and La show an increasing trend (Fig 7). Ce follows a state trend. In the P_2O_5 versus SiO_2, the Neshveh rocks demonstrate ascending trend that according to Chappell & White (1992) considered as an index of the «I-type» granites.

Chondrite-normalized REE pattern of the studied rocks have a little inclination and show low negative Eu anomaly (Fig 8). Normalizing these samples with primitive mantle, illustrates P, Nb and Ti negative anomaly and positive anomaly of K and Pb (Fig 9).

Discussion

Interpretation of the Geochemical and lithological results:

Journal of Academic and Applied Studies
(Special Issue on Applied Sciences)
Vol. 3(9) September 2013, pp. 22-37
Available online @ www.academians.org

Journal of Academic and Applied Studies

ISSN1925-931X

The Neshveh intrusive rock samples have high-K calk-alkaline nature (Fig 3) and so their linear trend in the AFM diagram indicate that the magma formed these rocks, simultaneously depleted from Fe and Mg and enriched of alkaline elements (Fig 4).

In the A/CNK versus A/NK diagram (shand, 1943) the studied rocks fall in the metaluminous field (Fig 3 and 5) propose their derivation from metamorphosed igneous rocks, lower crust or mantle wedge.

The major oxides amounts such as; TiO_2 ،MnO ،Fe_2O_3 and MgO have a decreasing trend with increasing SiO_2 due to their participation in the some ferromagnesian minerals structure like; pyroxene, hornblende, biotite and Fe-Ti oxides during magma fractionation. Al_2O_3 and CaO have a decreasing trend because of cooperation in the plagioclase structure. In the I-type granites, P behaves like a compatible element and is used for apatite formation. The P_2O_5 decreases with progress of the magma crystallization (Fig 6). Also quartz-monzodiorite to granite rock composition and presence of minerals such as; hornblende, sphene and lack of the muscovite and presence of metamorphosed minerals in the studied rocks all suppose the I-type rocks. K_2O and Na_2O increasing can be attributed as plagioclase (albite and orthoclase) crystallization during the latter stages of the magma crystallization. On the other hand, Rb and Ba increasing with SiO_2 can be caused from replacement of these elements with K in K-bearing minerals such as K-feldspar and biotite.

In the first stages of magma crystallization, Sr replaces Ca and enters into the Ca-bearing plagioclase net and hence gradually decreases in the magma. Due to big ionic radius and incompatibility, Th remains in the residual fluid of the last stages and increases with SiO_2. Y shows a decreasing trend that can be accounted for its entrance into the hornblende structure (Rollinson 1993; Willson 2007).

Sphene considered as the main host for Nb. Because of negligible amounts in the studied rocks, this element follows a state trend. Because of exiting from magma and entrance into the zircone structure in the first stages of the fractionation, Zr shows a descending trend in the rocks. Cr and Ni show conspicuous decreasing that indicate their compatibility and corporation into the ferromagnesian minerals net such as; pyroxene and olivine (Rollinson, 1993).

The igneous rocks of the studied area are sodic granites ($Na_2O>K_2O$) and have low amounts of Mg# ،Ni ،Cr ،Co and V. The low amounts of these elements can represent the high evolution of the magma during its ascending just before its complete solidification (Woodhead et.al., 1993).

Having similar trend for the REEs of the quartz-monzodiorite, granodiorite and granite normalized with Chondrite, same origin can be deduced (Boynton, 1984; Fig 8). Also their linear trend in the Y versus Yb diagram confirms this conclusion (Rollinson, 1993; Fig 10).

The low negative Eu anomaly (Fig 8) can imply the fractionation of feldspar during magma crystallization or its remaining in the source. Eu anomaly concomitant with Sr negative anomaly suggests plagioclase fractionation (Willson, 2007; and is related to the fractionation of Ca-bearing Plagioclases) as it can be observed in the studied rocks whereas Eu and Ba negative anomaly together point to K-feldspar fractionation.

Journal of Academic and Applied Studies
(Special Issue on Applied Sciences)
Vol. 3(9) September 2013, pp. 22-37
Available online @ www.academians.org

ISSN1925-931X

Ti, P, Ta, Nb and Ba show negative anomaly in the studied samples normalized with primitive mantle (Sun & McDonough, 1989) while Pb shows positive anomaly. Ti negative anomaly is controlled by Ti-bearing minerals such as; sphene, ilmenite, rutile and some of the amphiboles. With increasing the pressure, Ti-bearing minerals solubility in the fluids decreases (Glenn, 2004) and consequently these High Field Strength Elements (HFSE)-rich minerals remain as residual phases during partial melting in the depths more than 30 km and hence cause to negative anomaly in the melt (Glenn, 2004). Negative anomaly of P may results from low apatite values in the granodioritic rocks. As mentioned above in the I-type granites P behaves as a compatible element and its segregation in the initial stages of the magma fractionation made its negative anomaly in these rocks.

Metasomatism of the upper mantle prism by derived fluids from subducted oceanic crust yields Ta and Nb negative anomaly (Chappell, 1999).In the same way, according to Atherton and Ghani (2002) and Kamber et al., (2002) Pb positive anomaly in the samples can be justified.

The samples normalized with primitive mantle show LILE and LREE enrichment which implies the magma has formed in the subduction setting (Floyd &Winchestcr, 1994).

Tectonomagmatic Setting:

In order to determine the tectonic setting and magmatic characteristics of the Neshveh granodioritic mass, Pearce et al., (1996) diagram was used. Applying frequency logarithm of the trace elements including; Nb, Rb and Y in the vertices, these diagram is drawn and establish volcanic arc granodiorites for the Nevaeh intrusive mass (Fig 11) which is in agreement with some else geochemical evidences such as; decreasing trend of P_2O_5 with SiO_2 and so Nb and Ta negative anomaly.

Low values of Nb and Y relative to the mid oceanic ridge granites suggest more depleted mantle for these rocks as can be seen in the Pearce diagram. Lower contamination with the continental crust in comparison with sin-collisional granitesis assumed for lower amounts of Rb in these samples and their concentration below the sin-collisional granites field on this diagram.

Using Batchelor and Bowden (1985; Fig 12) and Harris et al.,(1986; Fig 13) the studied samples show Pre-collisional and volcanic arc setting respectively that are accordance with Pearce et al., (1996) diagrams.

Conclusions:

Based on field studies, petrographical and geochemical evidences quartzmonzodiorite to granite have been considered for Nehveh rock composition. The main effective factor in the evolution of the magma formed these rocks is crystal fractionation. Decreasing Al_2O_3, Fe_2O_3, MgO and CaO with increasing SiO_2 point to fractionation of plagioclase, amphibole and Fe-Ti oxides during magma fractionation. The Neshveh mass has calk-alkaline Metaluminous nature and show I-type granitoides characteristics. All evidences reveal that the studied mass formed

during subduction of Neotethyan oceanic crust beneath the central Iran in a volcanic arc geodynamic setting.

References

[1]- Ghalamghash, J. (1377). Saveh Geological Map Description (scale 1:100000), *Geological Survey of Iran.*

[2]- Helmi, F.,(1991).Petrology and Geochemistry of the igneous rocks in the Newshat area (northeast saveh), *M.Sc Thesis, Tehran university*

[3]- Alavi M.(1994).Tectonics of the Zagros Orogenic belt of Iran: new dataand interpretations. *Tectonophysics* 229: 211–238.

[4]- Atherton M.P.,and Ghani A.A. (2002).Slab breakoff: a model for Caledonian, Late Granite syncollisionalmagmatism in the orthotectonic (metamorphic) zone of Scotland and Donegal, Ireland. *Lithos62: 65–85.*

[5]- Berberian F.,and Berberian M.(1981).Tectono-plutonic episodes in Iran. In: Gupta, H.K., Delany, F.M. (Eds.), Zagros, Hindu Kush, Himalaya.*Geodynamic Evolution, American Geophysical Union, Geodynamics Series* 3: pp 5–32.

[6]- Berberian M.,and King, G.C.(1981).Towards a palaeogeography and tectonics evolution of Iran. *Canadian Journal of Earth Sciences 18: 210–265.*

[7]- Batchelor R A.,and Bowden P (1985).Petrogenetic interpretation of granitoid rock series using multicationic parameters. *ChemGeol* 48: 43-55.

[8]- Boynton W.V.(1984).Cosmochemistry of the rare earth elements: Meteorite studies, in Henderson, P., ed., Rare earth element geochemistry: HENDERSON P. (ed), Rare Earth Element Geochemistry, *Elsevier*, 63-114
.
[9]- Caillat C., Dehlavi P.,and Martel Jantin, B.(1978) .Geologie de la region de Saveh(Iran). Contribution a l'etude du volcanism et du plutonismtertiaresde la zone de I Irancentral(These de doctorat de specialities).

[10]- Chappell B.W.(1999).Aluminium saturation in I and S-type granites and the characterization of fractionated haplogranites. *Lithos*, 46: 535–551.

[11]- Chappell, B.W. and White, A.J.R.,(1992). I- and S-type granites in the Lachlan Fold Belt.Trans. *R. Soc. Edinburgh, Earth Sci.* 83, pp. 1–26.
[12]- Emami M.H.(1981).Geologie de la region de Qom-Aran (Iran);Contribution a petude dynamique et geochimique du Volcanisme tertiaire de l'Iran central. Theses. Sciences naturelles Univ. *Sc. Et Medicale de Grenobl*e.489p.

[13]- Floyd P.A. and Winchester J.A. (1994). Magma type and tectonic setting discrimination using immobile elements. *Earth Plan.* Sci. Let. 27:211-218.

[14]- Glenn A. G.(2004). The influence of melt structure on trace element partitioning near the peridotite solidus. *Contrib Mineral Petrol*, 147: 511–527

[15]- Harker A.(1909).The natural history of igneous rocks. *Methneu, London*.344p.

[16]- Harris N.B.W., Pearce J.A.,and Tindle A.G.(1986).Geochemical characteristics of collision zone magmatism. Collision tectonic.*Geological society of American Bulltein, special pub*. No. 19: 67–81.

[17]- Irvine, T.N.,and Baragar, W.R.A., (1971). A guide chemical classification of the common volcanic rock.*Canada, J. Earth Sci*, 8: 523–548.

[18]- Kamber B.S., Ewart A., Collerson K.D., Bruce M.C.,and McDonald G.D.(2002).Fluid-mobile trace element constraints on the role of slab melting and implications for Archaean crustal growth models. *Contrib Mineral Petrol*, 144: 38–56.

[19]- Moenvaziri H (1999). The Magmatism of Iran (in Farsi). Tarbiate-e-Moalem Univ., Tehran, 356 p..
[20]- Pearce J.A.(1996).Sources and settings of granitic rocks. *Episode* 19:120-125.

[21]- Peccerillo A.,and Taylor S.R.(1976). Geochemistry of Eocene calcalkalinevolkanic rocks from Kastamonu area, Northern Turkey*: Contrib.Mineral. Petrol*. 58: 63-81.

[22]- Rollinson H.(1993).Using geochemical data: Evaluation, presentation, interpretation. *Longman, Singapore*, p. 352.

[23]- Shahabpour J.(2007). Island-arc affinity of the central Iranian volcanic belt*: Journal of Asian Earth Sciences*, vol. 30: 652-665 p.

[24]- Shand S. J. (1943). Eruptive rocks, 2nd ed. John Wiley, New York, pp 1-444.

[25]- Sto¨cklin J.(1981). A brief report on geodynamics in Iran. In: Gupta, H.K.,Delany, F.M. (Eds.), Zagros, Hindu Kush, Himalaya. Geodynamic Evolution, *American Geophysical Union, Geodynamics Series*, vol. 3: pp. 70–74.

[26]- Stöcklin J.(1968). Structural history and tectonics of Iran; a review. *American Association of Petroleum Geologists Bulletin* 52:1229–1258.

[27]- Strekeisen A.L.,and Lemaitre R.W.(1979). A chemical approximation to the modal QAPF classification of the igneous rocks. *Neuse Jahrbuch fur MineralogieAb-handlunge*n. 136: 169–206.

[28]- Sun S.S.,and McDonough W.F.(1989). Chemical and isotopic systematics of oceanic basalts: implications for mantle composition and processes. In: Saunders A.D., Norry M.J. (Eds.), Magmatism in the Ocean Basins. *Geological Society Special Publication*, vol. 42, pp. 313–345.

[29]- Wilson M.(2007). Igneous Petrogenesis. *Chapman & Hall, London*. 411pp.

[30]- Woodhead J.D., Johnson R.W.,and troll,(1993). Isotop and trace element profile across the new Britain Island arc Papua new guines. *Contrib. M ineral. Petrol*.113:479-491.

Journal of Academic and Applied Studies
(Special Issue on Applied Sciences)
Vol. 3(9) September 2013, pp. 22-37
Available online @ www.academians.org

ISSN1925-931X

Table 1. Modal composition of the Neshveh rocks

	Qzmonzodiorite	***Granodiorite***					***granite***	
Sample No	SN10	SN11	SN15	SN17	SN31	SN48	SN44	SN52
SiO2 (wt %)	56.5	59.6	62.7	62.5	62.3	64	65.1	69.4
Quartz	11	17	20	20.5	20.4	21	24	29
K-feldspar	9.5	16.8	16	17.1	19	18	26	30
Plagioclase	53	44	43.8	43.6	43	42.5	39.2	35.4
Clinopyroxene	5	3	1	1.5	0.9	1.55	0.3	0.1
Hornblende	13	12	11.35	10.8	10.5	11	8	3
Biotite	5	5	5.5	3.7	4	3.8	0.5	1.5
Apatite	0.5	0.2	0.15	0.3	0.2	0.15	0	0
Opaque	3	2	2.2	2.5	2	2	2	1
Sum	100	100	100	100	100	100	100	100

Journal of Academic and Applied Studies
(Special Issue on Applied Sciences)
Vol. 3(9) September 2013, pp. 22-37
Available online @ www.academians.org

ISSN1925-931X

Table2. Major and trace element abundances in selected samples of the Neshveh rocks

Sample No	SN05	SN10	SN11	SN15	SN17	SN31	SN44	SN48	SN52
SiO_2	49	56.5	59.6	62.7	62.5	62.3	65.1	64	69.4
Al_2O_3	14.65	17.1	16.7	16.15	15.45	15.75	14.8	15.65	13.8
Fe_2O_3	13.4	8.66	7.66	6.03	5.07	5.98	3.89	5.17	3.05
CaO	7.89	7.16	5.89	4.81	3.38	4.15	4.84	3.8	2.27
MgO	5.09	3.26	2.48	1.78	2.05	2.58	1.52	1.98	1.1
Na_2O	4.28	3.23	3.59	3.49	3.64	3.36	3.47	3.41	3.06
K_2O	1.14	1.85	2.31	2.73	3.46	2.95	2.9	3.26	4.19
TiO_2	1.12	0.73	0.71	0.57	0.51	0.59	0.49	0.53	0.32
MnO	0.22	0.14	0.14	0.15	0.13	0.1	0.05	0.09	0.07
P_2O_5	0.15	0.23	0.2	0.19	0.15	0.19	0.15	0.16	0.09
SrO	0.03	0.06	0.05	0.05	0.04	0.05	0.05	0.04	0.03
BaO	0.04	0.06	0.07	0.09	0.08	0.06	0.1	0.07	0.09
LOI	0.09	0.77	0.48	1.09	1.56	1.38	0.89	1.37	1.37
Ba	354	465	548	675	701	618	759	665	808
Ce	39.5	28.4	30.8	45.7	32.6	25.6	31.6	26.6	34.9
Cr	15.9	23.8	17.4	12.8	8	12	5	10.2	4
Ce	40	20	10	10	<10	10	10	10	<10
Cs	0.71	1.95	2.34	1.22	1.49	1.19	0.4	1.74	1.47
Cu	18	53	48	47	22	59	5	17	8
Dy	4.14	3.73	4	3.48	3.88	3.22	3.26	3.56	2.8
Er	2.53	2.18	2.45	2.12	2.41	1.99	2.12	2.28	1.89
Eu	1.53	0.99	0.94	0.95	0.91	0.98	0.88	0.9	0.6
Ga	17.6	17.5	17.7	16.2	15	15.3	14.4	15.3	13.2
Gd	3.77	3.67	3.87	3.91	4.15	3.4	3.65	3.69	2.99
Hf	2.3	2.4	3.5	3.6	3.8	3.1	4.1	4.1	3.8
Ho	0.83	0.77	0.8	0.71	0.83	0.66	0.69	0.74	0.6
La	23.2	14	15.3	24.2	16.8	13.1	16	13.1	19.7
Lu	0.39	0.33	0.4	0.36	0.37	0.29	0.33	0.66	0.34
Nb	1.5	4.8	6.6	6.6	7.9	6.5	7.4	8.2	8.7
Nd	13.2	14.9	15.4	19.3	16.2	13.3	14.9	14.2	14.2
Ni	19	14	8	8	<5	6	5	<5	<5
Pb	<5	7	11	13	21	10	6	15	17
Pr	3.93	3.64	3.85	5.24	4.07	3.3	3.85	3.53	3.9
Rb	29.5	48.7	60.9	71.4	74.2	63.5	38.1	78.2	90.8
Sm	2.9	3.38	3.53	3.76	3.7	3.1	3.21	3.43	2.84
Sn	8	2	1	1	1	1	2	1	1
Sr	271	503	424	449	347	381	353	352	248
Ta	0.1	0.3	0.5	0.5	0.5	0.5	0.5	0.5	0.7
Tb	0.62	0.59	0.56	0.56	0.64	0.54	0.55	0.59	0.46
Th	0.35	3.17	5.55	5.55	5.89	4.98	5.91	6.18	8.42

Journal of Academic and Applied Studies
(Special Issue on Applied Sciences)
Vol. 3(9) September 2013, pp. 22-37
Available online @ www.academians.org

ISSN1925-931X

Tm	0.36	0.32	0.34	0.32	0.37	0.29	0.32	0.34	0.29
U	1.87	0.71	1.23	1.43	1.3	1.05	1.56	0.97	1.78
V	506	241	194	128	89	118	76	87	47
W	1	1	2	2	2	2	1	2	1
Y	22	20.9	23	20.4	21.6	17.5	18.4	19.7	16.2
Yb	2.37	2.24	2.39	2.14	2.44	1.93	2.16	2.29	2.06
Zn	98	51	75	76	80	40	23	51	44
Zr	81	83	119	121	134	113	145	145	124

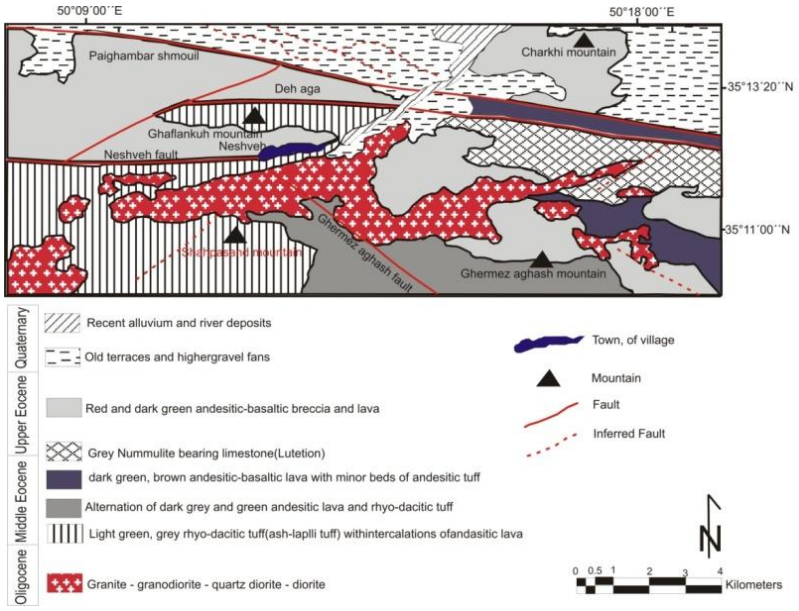

Fig. 1.Geological map of the Neshveh area (after Ghalamghash, 1998).

Journal of Academic and Applied Studies
(Special Issue on Applied Sciences)
Vol. 3(9) September 2013, pp. 22-37
Available online @ www.academians.org

ISSN1925-931X

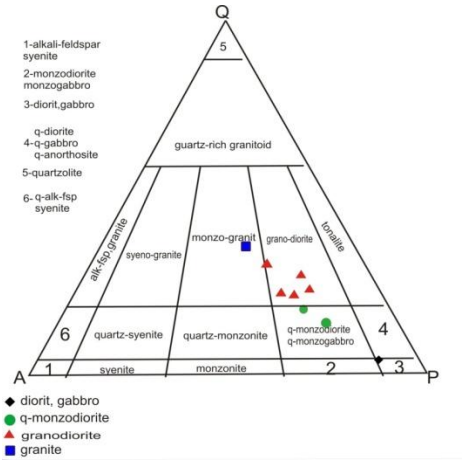

Fig. 2. Modal analysis results of the studied samples plotted on the Strekeisen (1979) diagram. Q= quartz%, A=alkaline feldspar%, P=plagioclase%

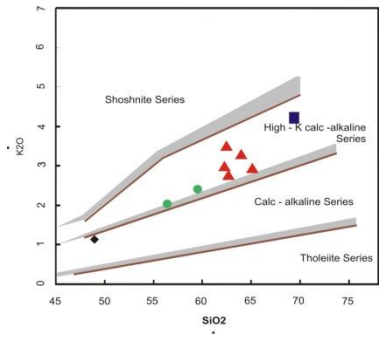

Fig. 3. K_2O vs. SiO_2 discrimination diagram (Peccerillo and Taylor, 1976); in this diagram most of samples plot in the High-K calc-alkaline series. Symbols are the same as for Fig. 2

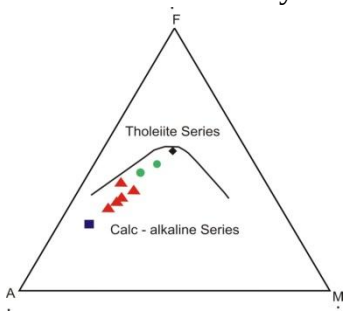

Fig. 4. AFM diagram after Irvine and Baragar (1971). The Neshveh intrusive mass delineate a calc-alkaline trend. Symbols are the same as for Fig. 2

Journal of Academic and Applied Studies
(Special Issue on Applied Sciences)
Vol. 3(9) September 2013, pp. 22-37
Available online @ www.academians.org

ISSN1925-931X

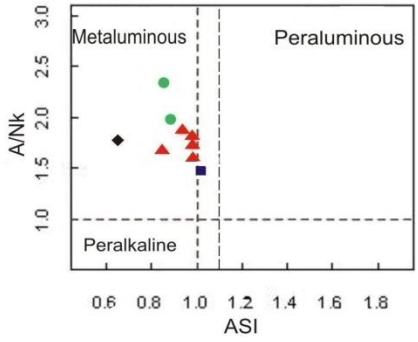

Fig. 5. A/CNK versus A/NK Shand index diagram (Maniar and Piccolli, 1989). In this diagram the samples plot in the metaluminous field. Symbols are the same as for Fig. 2

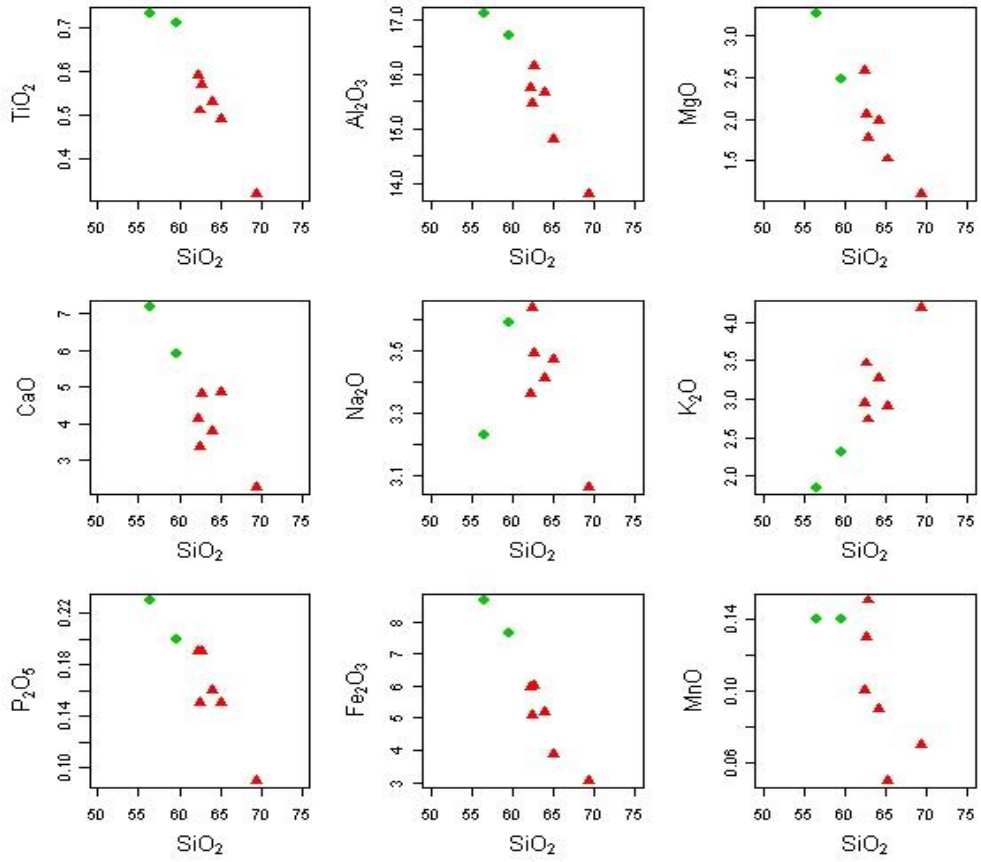

Fig. 6. Selected SiO_2 versus major oxide (wt%) plots for the studied mass. Symbols are the same as for Fig. 2

Journal of Academic and Applied Studies
(Special Issue on Applied Sciences)
Vol. 3(9) September 2013, pp. 22-37
Available online @ www.academians.org

ISSN1925-931X

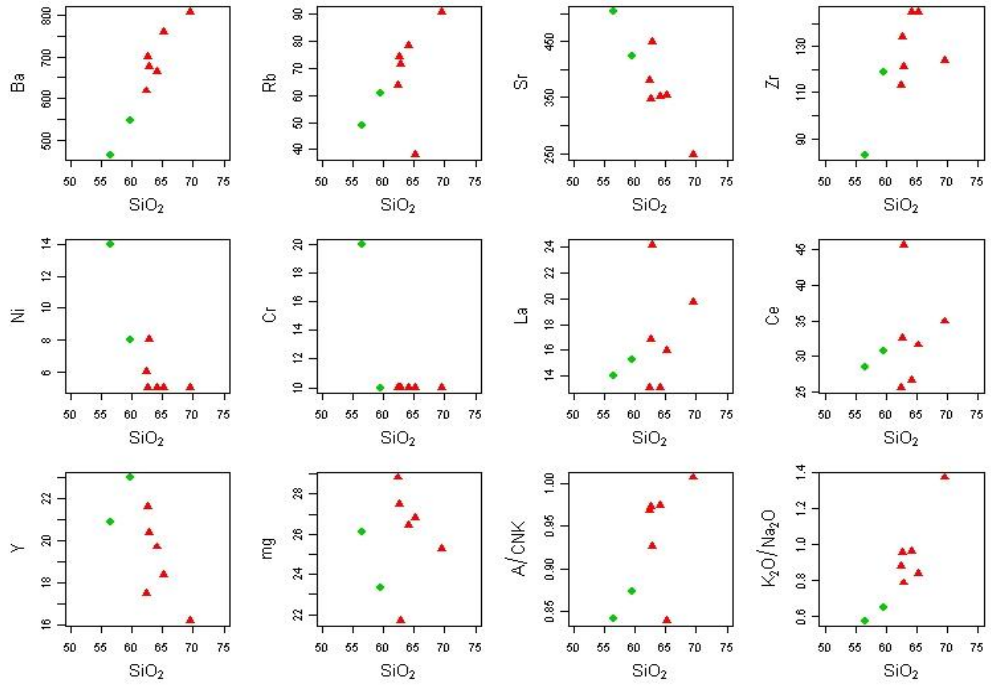

Fig. 7. Chemical variation diagrams for trace elements (in ppm) of the Neshveh intrusive rocks. Symbols are the same as for Fig. 2

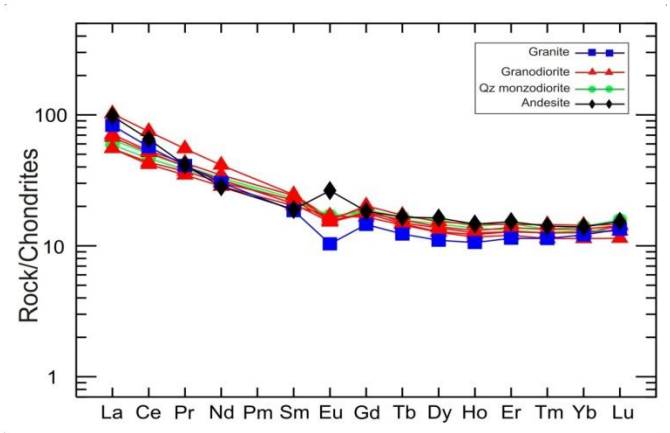

Fig. 8. Chondrite normalized REE variation for Neshveh rocks. Symbols are the same as for Fig. 2

Journal of Academic and Applied Studies
(Special Issue on Applied Sciences)
Vol. 3(9) September 2013, pp. 22-37
Available online @ www.academians.org

ISSN1925-931X

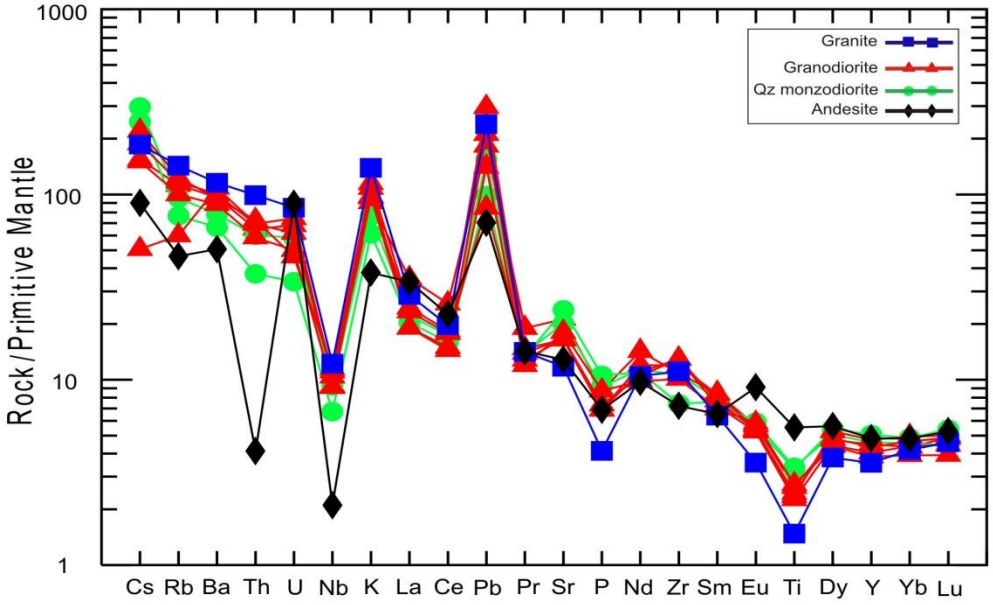

Fig. 9. Primitive mantle normalized trace element variation of the selected samples. Normalizing values from Sun and McDonough (1989). Symbols are the same as for Fig. 2

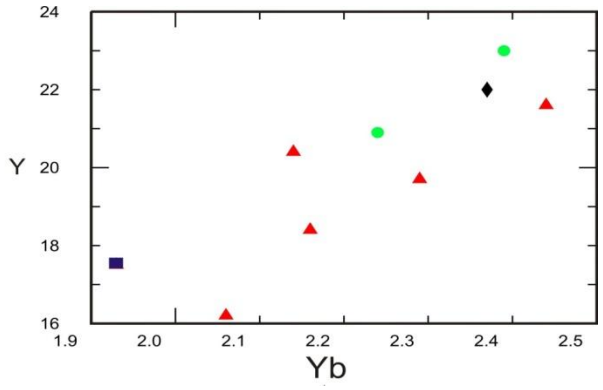

Fig. 10. Y vs. Yb variation diagram. The linear trend represents their unity source. Symbols are the same as for Fig. 2

Journal of Academic and Applied Studies
(Special Issue on Applied Sciences)
Vol. 3(9) September 2013, pp. 22-37
Available online @ www.academians.org

ISSN1925-931X

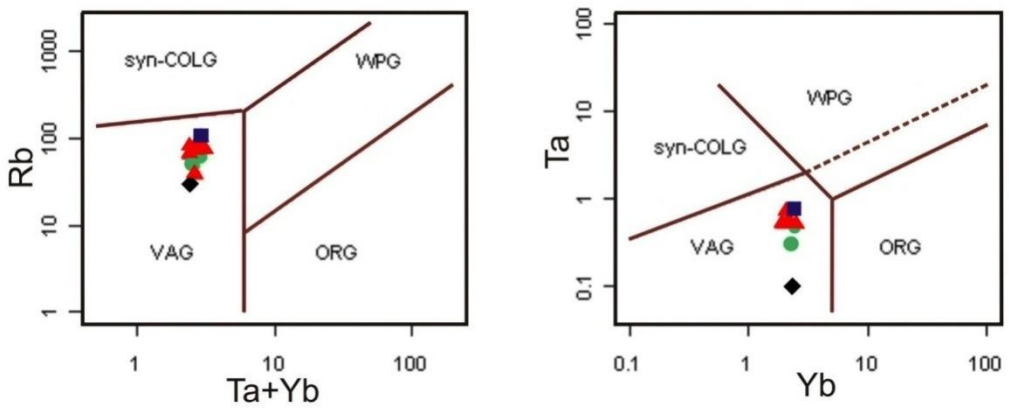

Fig. 11. Tectonic discrimination diagram from Pierce et al., (1996) representing VAG setting for the Neshveh rocks. Symbols are the same as for Fig. 2

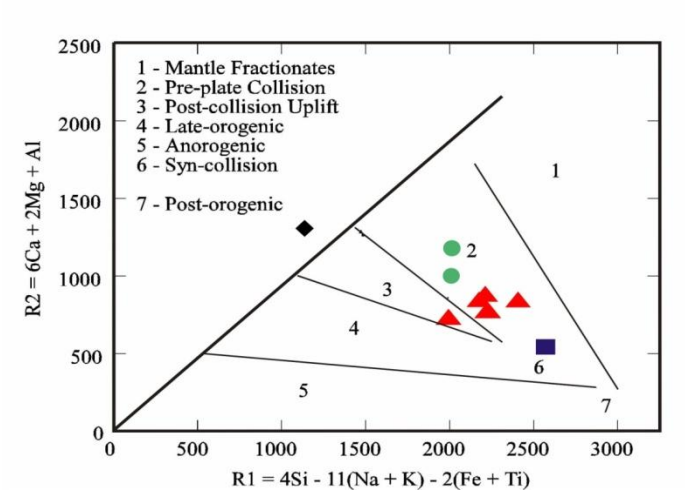

Fig. 12. R1–R2 major element geotectonic discrimination diagram (Batchelor and Bowden, 1985). Symbols are the same as for Fig. 2

Journal of Academic and Applied Studies
(Special Issue on Applied Sciences)
Vol. 3(9) September 2013, pp. 22-37
Available online @ www.academians.org

ISSN1925-931X

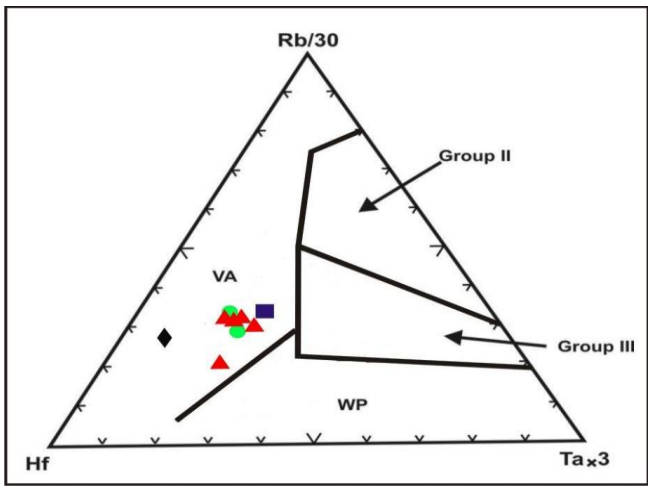

Fig. 13. Rb/30-Hf-Ta×3 ternary diagram showing that the whole of the samples plot within the volcanic arc (VA) field (Harris, 1986). Symbols are the same as for Fig. 2